Japanese Journal of Applied Physics
Vol. 44, No. 6B, 2005, pp. 4609–4614

Frequency Analysis of Strain of Cylindrical Shell for Assessment of Viscosity

Hideyuki HASEGAWA* and Hiroshi KANAI

Graduate School of Engineering, Tohoku University, Sendai 980-8579, Japan

(Received November 11, 2004; accepted March 30, 2005; published June 24, 2005)

For tissue characterization of atherosclerotic plaque, we have developed a method, namely, the *phased tracking method*, [H. Kanai *et al.*: IEEE Trans. Ultrason. Ferroelectr. Freq. Control **43** (1996) 791] to measure the regional strain (change in wall thickness) and elasticity of the arterial wall. In addition to the regional elasticity, we are attempting to measure the regional viscosity for a more precise tissue characterization. Previously, we showed that the viscosity can be obtained by measuring the frequency dependence of the elastic modulus using remote actuation [H. Hasegawa *et al.*: Jpn. J. Appl. Phys. **43** (2004) 3197]. However, in this method, we need to apply external actuation to the subject. To simplify the measurement, we instead to obtain the frequency dependence of the elastic modulus from the change in arterial wall thickness spontaneously caused by the heartbeat because this change in thickness consists of frequency components up to 20–30 Hz. In this paper, the frequency dependence of the elastic modulus of a silicone rubber tube was investigated by applying frequency analysis to the change in wall thickness caused by the change in internal pressure simulating the actual arterial blood pressure.
[DOI: 10.1143/JJAP.44.4609]

KEYWORDS: change in wall thickness, frequency characteristics, viscoelasticity, atherosclerosis

1. Introduction

There are significant differences between the elastic moduli of a normal arterial wall and those affected by atherosclerosis.[1,2] Therefore, evaluation of the elasticity of the arterial wall is useful for diagnosis of atherosclerosis.[3] In particular, mechanical properties of plaque are important because the rupture of the plaque may cause acute myocardial infarction and cerebral infarction.[4–6] However, the mechanical properties, such as elasticity, of plaque itself cannot be noninvasively measured by previous methods[7–9] on the basis of the measurement of the change in diameter of the artery caused by a heartbeat.[10–14]

For assessment of the regional elasticity of plaque itself, we have developed a method, namely, the *phased tracking method*, for measurement of the small change in thickness of the arterial wall (less than 100 μm) due to the heartbeat.[15–23] From basic experiments, the accuracy in measurement of the change in thickness has been found to be less than 1 μm using the *phased tracking method*.[16,19,20] From the change in thickness measured by our method, the regional strain and the elasticity of the arterial wall can be noninvasively evaluated.[22,24]

From the measured elastic property, it should be possible to discriminate tissues in the atherosclerotic plaque, such as fibrous tissue and lipids, due to large differences in their elasticities. However, it is difficult to discriminate some tissues because of their small difference in elasticity. One of the additional mechanical properties of tissues which has a potential to provide useful information on discrimination of tissues is viscosity.

We showed that the viscosity can be estimated based on the measurement of the elastic moduli at multiple frequencies by applying external actuation.[25,26] To obtain the regional elastic moduli at multiple frequencies, it is necessary to generate the change in diameter (=change in internal pressure) instead of the bending vibration of the artery. However, it is not easy to stably generate the change in internal pressure using remote actuation. To overcome this problem and simplify the measurement procedure, measurement of the frequency characteristics without external actuation is desired. It is reported that the rapid increase in blood pressure in the early systole, which is caused by contraction of the left ventricle, has frequency components up to 20–30 Hz.[27] However, there is a large increase in blood pressure of typically 50 mmHg. Due to such a large increase in blood pressure, the viscoelasticity estimation is largely influenced by the nonlinearity of the stress–strain relationship of the wall. To overcome this problem, we focused on the rapid decrease in blood pressure in the late systole. This pressure decrease is caused by the following mechanism: Blood supply is stopped by closure of the aortic valve. However, blood tends to flow away to the periphery due to the inertia of blood. Then, blood pressure decreases. In this stage, the absolute value of the change in blood pressure is much smaller than that in the early systole, and the influence of the nonlinearity can be assumed to be negligible. In this paper, basic experiments using a silicone rubber tube were conducted to measure the viscosity of a cylindrical shell by applying frequency analysis to the change in wall thickness caused by a sophisticated flow pump that can simulate the change in arterial blood pressure.

2. Principles

2.1 Frequency analysis of change in wall thickness measured with ultrasound

The change in wall thickness, $\Delta h(t)$, caused by the change in internal pressure, $\Delta p(t)$, can be measured by the *phased tracking method*,[15] which uses the phase shift of echoes reflected by a moving object. For assessment of the frequency dependence of the elastic modulus of the wall, frequency analysis was applied to the measured changes in wall thickness, $\Delta h(t)$, and internal pressure, $\Delta p(t)$, to obtain their amplitudes, $\Delta h_0(f)$ and $\Delta p_0(f)$, at a frequency f. Figure 1(b) shows the velocity of the carotid arterial wall of a 30-year-old male for seven heartbeats measured by the *phased tracking method*. Figure 1(c) shows the displacement of the posterior wall obtained by integrating the measured velocity. Figure 1(d) shows the power spectra of the velocities during periods (A) and (B) obtained by applying

*E-mail address: hasegawa@us.ecei.tohoku.ac.jp

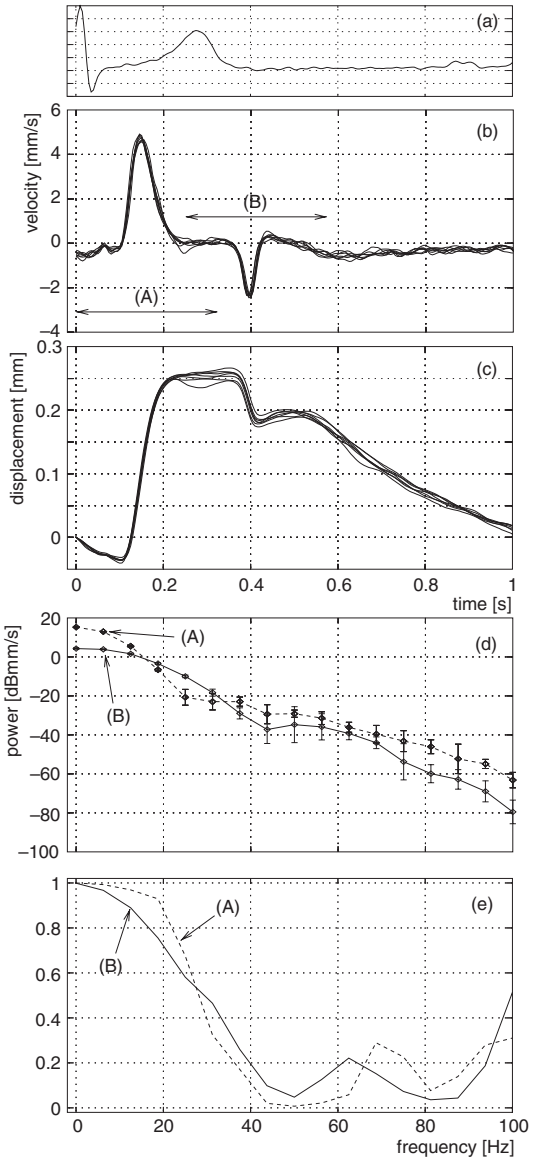

Fig. 1. Vibration of human carotid arterial wall caused by heartbeat. (a) Electrocardiogram. (b) Velocities of wall for seven heartbeats measured by *phased tracking method*.[15] (c) Wall displacements obtained by integrating velocities. (d) Power spectra of velocities during periods (A) and (B). (e) Reproducibility functions.

the Fourier transform. Plots and vertical bars show means and standard deviations for seven heartbeats, respectively. Furthermore, Fig. 1(e) shows the reproducibility function.[15] If the reproducibility function is one at a certain frequency, f, the amplitude and phase of the frequency component at f are identical for seven heartbeats. As shown in Fig. 1(e), the rapid motion in the early systole, which is indicated as period (A) in Fig. 1(b), was measured with respect to frequency components up to 20 Hz with good reproducibility. However, there is a large increase in internal pressure of typically 50 mmHg. For the subject shown in Fig. 1, the blood pressure was increased from 60 mmHg to 110 mmHg during period (A) of about 100 ms. To obtain the frequency spectrum from 5 Hz to 20 Hz, the required length of the time window for the frequency analysis is at least 200 ms, which corresponds to one wavelength of the 5 Hz components. Therefore, the rapid increase in blood pressure from 60 mmHg to 110 mmHg for 100 ms is included in the analyzing period. It was reported that the stress-strain relationship of the arterial wall is nonlinear.[28] This fact means that the viscoelasticity of the arterial wall itself is modified by the change in internal pressure corresponding to the stress acting on the wall. The viscoelasticity of the wall is expressed by the complex elastic modulus. The real and imaginary parts correspond to the static elastic modulus, E_s, and the viscous term, $2\pi f\eta$, respectively. No data on the pressure dependence of the arterial-wall viscosity, η, has yet been presented in the literature. The pressure dependence of the static elastic modulus, E_s, of the carotid artery was reported to be from 0.4 MPa to 1.1 MPa (from 60 mmHg to 110 mmHg).[28] The viscosity of the carotid arterial wall is reported to be about 5 kPa·s,[28] and the viscous component, $2\pi f\eta$, changes from 0 to 0.6 MPa (from direct current to 20 Hz). The change in static elastic modulus due to the change in blood pressure is comparable to the change in the viscous component with respect to frequency. Therefore, from the measured elastic modulus, which corresponds to the absolute value of the complex elastic modulus, it is difficult to distinguish the frequency dependence from the pressure (or stress) dependence during period (A).

We can find another pulsive velocity in the late systole shown by period (B) in Fig. 1(b). From the wall displacement shown in Fig. 1(c), the decrease in blood pressure is expected to be from 110 mmHg to 100 mmHg during period (B). This change in internal pressure is much smaller than that in the early systole, and the change in elasticity was reported to be from 1.1 MPa to 1.0 MPa.[28] Therefore, it can be assumed that only the frequency dependence of the elastic modulus can be obtained in this timing. As shown in Fig. 1(e), it was found that frequency components up to at least 10 Hz can be measured with good reproducibility. From these results, the pulsive velocity of the wall in the late systole has a potential for measurement of the frequency dependence of the elastic modulus.

In this study, a change in internal pressure similar to that at the human carotid artery was generated by a sophisticated flow pump. The resultant change in internal pressure and the wall thickness of a silicone rubber tube were measured with a pressure transducer and ultrasound. The frequency dependence of the elastic modulus was obtained by applying frequency analysis to the vibration corresponding to that of the arterial wall in the late systole.

2.2 *Elastic modulus obtained by measured change in wall thickness*

From the measured change in wall thickness, the circumferential elastic modulus is obtained as follows:[22] Under *in vivo* conditions, the artery is strongly restricted in the axial direction. Therefore, a two-dimensional stress-strain relationship can be assumed.

Under such conditions, the radial incremental strain, $\Delta\varepsilon_r(t)$, which is defined by dividing the change in thickness, $\Delta h(t)$, by the original thickness of the wall, h_0, at the end diastole, is expressed by the radial and circumferential incremental stresses, $\Delta\sigma_r(t)$ and $\Delta\sigma_\theta(t)$, as follows:

$$\Delta\varepsilon_r(t) = \frac{\Delta h(t)}{h_0}$$

$$= \frac{\Delta\sigma_r(t)}{E_r} - \nu\frac{\Delta\sigma_\theta(t)}{E_\theta}, \tag{2.1}$$

where E_r, E_θ, and ν are the radial and circumferential elastic moduli and Poisson's ratio, respectively.

From the change in internal pressure, $\Delta p(t)$, the circumferential and radial incremental stresses, $\Delta\sigma_r(t)$ and $\Delta\sigma_\theta(t)$, are respectively expressed as follows:

$$\Delta\sigma_\theta(t) = \frac{r_0}{h_0}\Delta p(t), \tag{2.2}$$

$$\Delta\sigma_r(t) = -\frac{1}{2}\Delta p(t), \tag{2.3}$$

where r_0 is the inner radius at the end diastole.

By substituting eqs. (2.2) and (2.3) into eq. (2.1), eq. (2.1) is rewritten as follows:

$$\Delta\varepsilon_r(t) = -\frac{1}{2}\frac{\Delta p(t)}{E_r} - \nu\frac{r_0}{h_0}\frac{\Delta p(t)}{E_\theta}. \tag{2.4}$$

By assuming that the arterial wall is incompressible ($\nu \approx 0.5$) and elastically isotropic ($E_r \approx E_\theta$),[22,29] the elastic modulus, E_θ^h, obtained from the change in wall thickness is defined as follows:

$$E_\theta^h = \left(\nu\frac{r_0}{h_0} + \frac{1}{2}\frac{E_r}{E_\theta}\right)\frac{\Delta p(t)}{-\Delta\varepsilon_r(t)} \approx \frac{1}{2}\left(\frac{r_0}{h_0}+1\right)\frac{\Delta p(t)}{-\dfrac{\Delta h(t)}{h_0}}. \tag{2.5}$$

When we describe a frequency component of changes in wall thickness and internal pressure at a frequency f by $\Delta h_0(f)\cdot e^{j[2\pi ft-\psi(f)]}$ and $\Delta p_0(f)\cdot e^{j2\pi ft}$, eq. (2.5) is rewritten as the complex elastic modulus as follows:

$$E_\theta^h(f) = \frac{1}{2}\left(\frac{r_0}{h_0}+1\right)\frac{\Delta p_0(f)}{\dfrac{\Delta h_0(f)}{h_0}}\cdot e^{j\psi(f)}, \tag{2.6}$$

where $\Delta h_0(f)$ and $\Delta p_0(f)$ are the amplitude of the change in wall thickness and that of the change in internal pressure, respectively, and $\psi(f)$ is the phase delay of the change in wall thickness from the change in internal pressure at frequency f.

The imaginary part of the complex elastic modulus, which depends on the viscosity, has a frequency dependence. Therefore, both the absolute value, $|E_\theta^h(f)|$, and the phase, $\psi(f)$, of the complex elastic modulus have frequency dependences. However, particularly under an *in vivo* condition, it is difficult to measure the change in internal pressure, $\Delta p(t)$, at the exact same point where the change in wall thickness, $\Delta h(t)$, was measured. Therefore, the phase, $\psi(f)$, of the complex elastic modulus cannot be estimated. In this paper, the absolute value, $|E_\theta^h(f)|$, of the complex elastic modulus defined by eq. (2.6) is obtained from $\Delta h_0(f)$ and $\Delta p_0(f)$, which are obtained at each frequency f.

2.3 Viscoelasticity estimation using the Voigt model

In our previous study,[25] it was found that the elastic modulus, $|E_\theta^h(f)|$, of the arterial wall increases with frequency f. The reason for this is explained as follows.

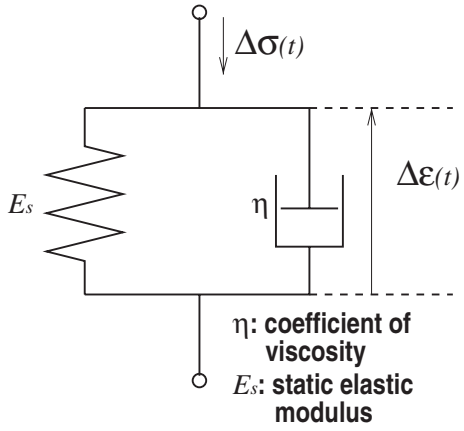

Fig. 2. Voigt model.

When we assume the Voigt model, which is illustrated in Fig. 2, as a viscoelastic model of the wall, the relationship between the stress, $\Delta\sigma(t)$, and the strain, $\Delta\varepsilon(t)$, is expressed as follows:

$$\Delta\sigma(t) = E_s\cdot\Delta\varepsilon(t) + \eta\cdot\frac{d}{dt}\Delta\varepsilon(t), \tag{2.7}$$

where E_s and η are the static elastic modulus and the viscosity constant, respectively, and E_s and η are assumed not to be changed by frequency.

By defining the frequency components at a frequency f by $\Delta\sigma(t;f) = \Delta\sigma_0(f)\cdot e^{j2\pi ft}$ and $\Delta\varepsilon(t;f) = \Delta\varepsilon_0(f)\cdot e^{j[2\pi ft-\psi(f)]}$, eq. (2.7) can be rewritten as

$$\Delta\sigma(t;f) = E_s\cdot\Delta\varepsilon(t;f) + j2\pi f\eta\cdot\Delta\varepsilon(t;f), \tag{2.8}$$

where $\Delta\sigma_0(f)$ and $\Delta\varepsilon_0(f)$ are the amplitudes of the stress and strain, respectively.

From eq. (2.8), the complex elastic modulus, $E_{Voigt}(f) = |E_{Voigt}(f)|e^{j\psi(f)} = \Delta\sigma(t;f)/\Delta\varepsilon(t;f)$, is given by

$$|E_{Voigt}(f)| = \sqrt{E_s^2 + (2\pi f\eta)^2}, \tag{2.9}$$

$$\psi(f) = \tan^{-1}\left(\frac{2\pi f\eta}{E_s}\right). \tag{2.10}$$

In this paper, the viscosity constant, η, and the static elastic modulus, E_s, were determined so as to minimize the difference between the measured $|E_\theta^h(f)|$ and the model-based $|E_{Voigt}(f)|$.

3. Experimental Setup

3.1 Experimental system for basic experiments

The experimental system for basic experiments using a silicone rubber tube is illustrated in Fig. 3. In this system, the change in pressure inside the silicone rubber tube was generated by a sophisticated flow pump (Shelly Medical Systems, CompuFlow1000). The change in wall thickness due to the resulting change in internal pressure was measured with ultrasound, and the internal pressure was also measured by a pressure transducer (NEC, 9E02-P16) placed inside the tube. From measured changes in the wall thickness and internal pressure, the elastic modulus was obtained using eq. (2.6).

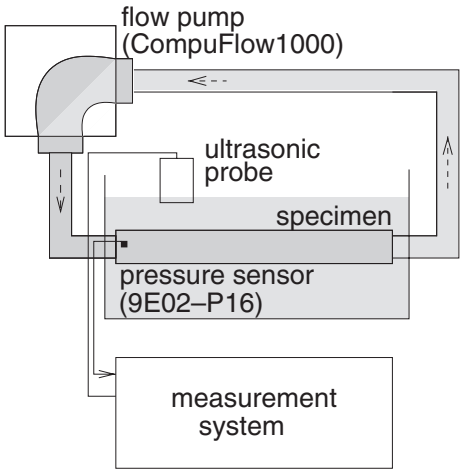

Fig. 3. Experimental setup.

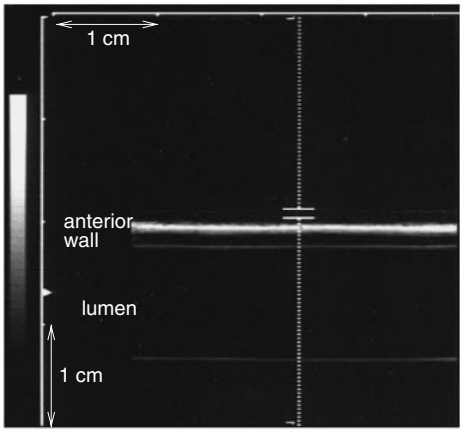

Fig. 4. B-mode image of silicone rubber tube.

3.2 *Measurement system*

An ultrasonic pulse (center frequency: 7.5 MHz) was transmitted and received by the ultrasonic probe of a standard ultrasonic diagnostic apparatus (Toshiba SSH-140A). The received signal was amplified and demodulated. The resultant in-phase and quadrature signals were simultaneously A/D converted by a 12-bit A/D converter at a sampling frequency of 10 MHz. The measured digital signals were transfered to a computer, and the change in wall thickness was obtained by applying the *phased tracking method*[15] to these digital signals.

4. Basic Experiments Using a Silicone Rubber Tube

Figure 4 shows the B-mode image of a silicone rubber tube. The M-mode image was obtained along an ultrasonic beam, as shown in Fig. 5(a). Figure 5(c) shows the measured internal pressure. From Fig. 5(c), it was found that the change in internal pressure, which is similar to that in the human artery, was generated by the flow pump. By setting two points, A and B, along the ultrasonic beam at a time $t = 0$ in the M-mode image, the velocities, $v_A(t)$ and $v_B(t)$, of these points were obtained by the *phased tracking method*, as shown in Figs. 5(e) and 5(f), respectively. The change in thickness of the posterior wall was obtained by integrating the difference between $v_A(t)$ and $v_B(t)$, as shown in Fig. 5(h).

Then, the amplitude, $\Delta h_0(f)$, of the measured change in wall thickness at a frequency f was obtained by applying the Fourier transform to the rate of the change in wall thickness, $\Delta\dot{h}(t) = v_B(t) - v_A(t)$, shown in Fig. 5(g). A Hanning window with a length of 200 ms was applied to the period shown in Fig. 5(g). Together with the change in wall thickness, the amplitude, $\Delta p_0(f)$, of the measured change in internal pressure shown in Fig. 5(c) was obtained from the "rate" of the change in internal pressure $\Delta\dot{p}(t)$. The direct current component of the change in internal pressure is much larger than the alternating current components, and the Hanning window with the length of 200 ms has a main lobe with a half bandwidth of ±5 Hz in the frequency domain. Therefore, the large direct current component affects the estimated frequency spectra at the other frequency. To remove this direct current component, the change in internal pressure, $\Delta p(t)$, was differentiated with respect to time before applying the Fourier transform. From the amplitudes, $\Delta\dot{h}_0(f)$ and $\Delta\dot{p}_0(f)$, of $\Delta\dot{h}(t)$ and $\Delta\dot{p}(t)$ estimated at each frequency f, $\Delta h_0(f)$ and $\Delta p_0(f)$ were obtained as follows:

$$\Delta h_0(f) = \frac{\Delta\dot{h}_0(f)}{2\pi f}, \tag{4.1}$$

$$\Delta p_0(f) = \frac{\Delta\dot{p}_0(f)}{2\pi f}. \tag{4.2}$$

Figure 6(a) shows the power spectra of rates of changes in wall thickness, $\Delta\dot{h}(t)$, and internal pressure, $\Delta\dot{p}(t)$. Plots and vertical bars show means and standard deviations for eleven beats, respectively. Figure 6(b) shows the reproducibility functions. In Fig. 6(b), it was found that both changes in wall thickness and internal pressure were measured with good reproducibilities up to 30 Hz. The elastic modulus, $|E^h_\theta(f)|$, was obtained from $\Delta h_0(f)$ and $\Delta p_0(f)$ for eleven beats, as shown in Fig. 7. In Fig. 7, the frequency characteristics of the elastic modulus were measured three times for the same silicone rubber tube (eleven beats for each measurement). Plots and vertical bars show means and standard deviations of the elastic moduli measured for eleven beats, respectively. In the frequency range under 10 Hz, where the reproducibility function is almost one, it was found that the elastic modulus, $E^h_\theta(f)$, was measured with sufficient reproducibility and $E^h_\theta(f)$ increased with frequency f. Such frequency characteristics can be explained by the Voigt model. Therefore, from the frequency characteristics under 10 Hz, the viscosity constant, η, and the static elastic modulus, E_s, were determined by applying the Voigt model. In Fig. 7, the estimated Voigt models are shown by solid curves, and the estimated parameters, η and E_s, for each measurement were the following: first measurement, 7.2 kPa·s and 2.2 MPa; second, 6.8 kPa·s and 2.1 MPa; and third, 7.6 kPa·s and 2.1 MPa. These values were in good agreement with $\eta = 6.46$ kPa·s and $E_s = 2.26$ MPa obtained by the different mechanical test (Shimadzu, Tritech2000) in which the amplitude and phase of the strain generated by the applied sinusoidal stress was measured for a string extracted from the silicone rubber tube. In this mechanical testing, E_s was not obtained from the static experiment, and a sinusoidal stress at a frequency of 5 Hz, which corresponds to the center of the frequency range for the estimation of E_s and η in the

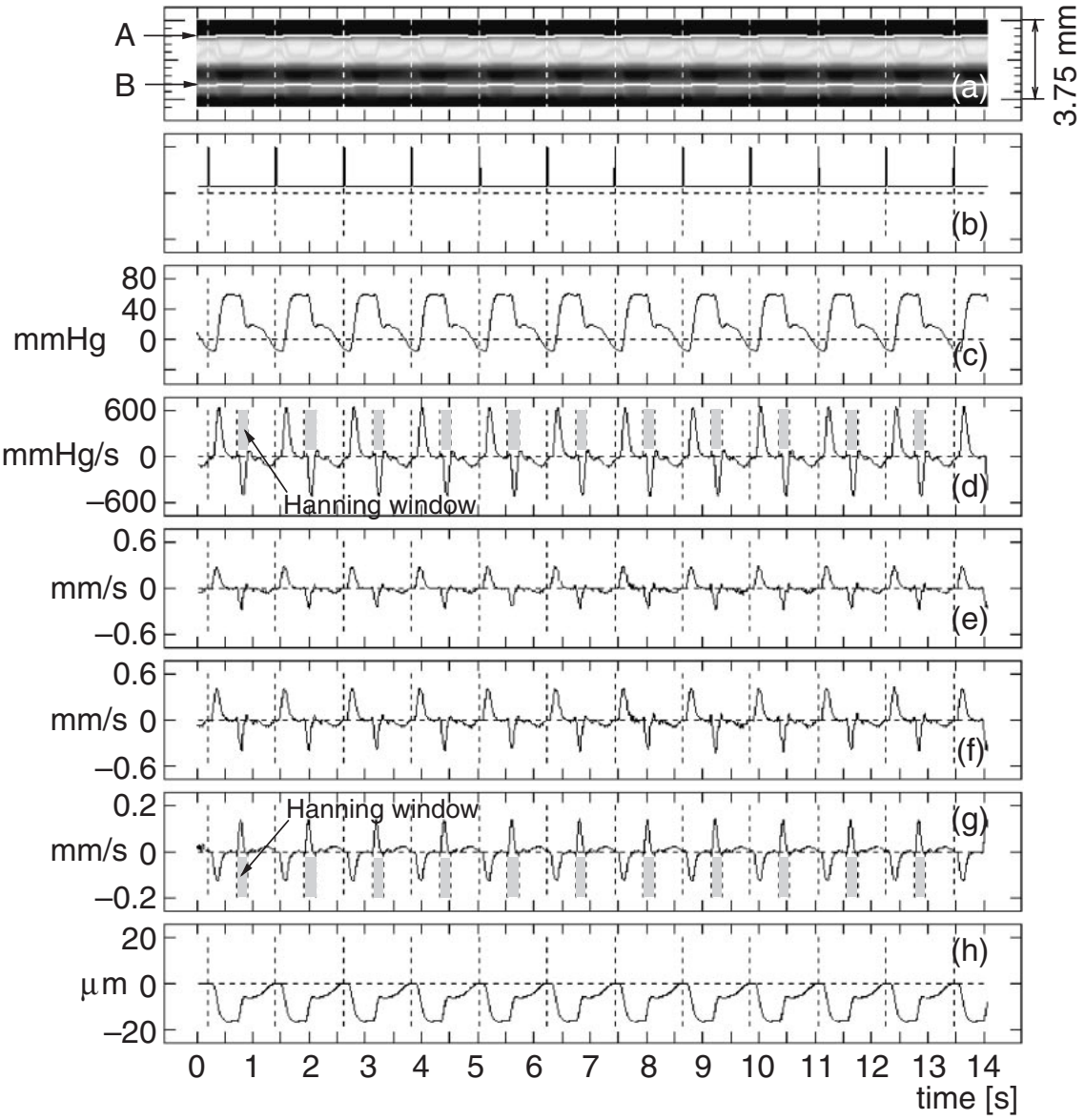

Fig. 5. (a) M-mode image of silicone rubber tube. (b) Drive signal of flow pump. (c) Internal pressure. (d) Rate of internal pressure. (e) Velocity at A. (f) Velocity at B. (g) Rate of change in thickness of anterior wall. (h) Change in wall thickness.

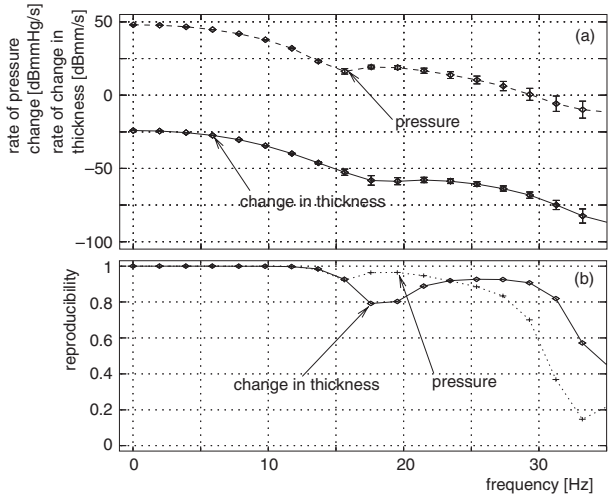

Fig. 6. (a) Power spectra of rates of changes in internal pressure and wall thickness. (b) Reproducibility functions.

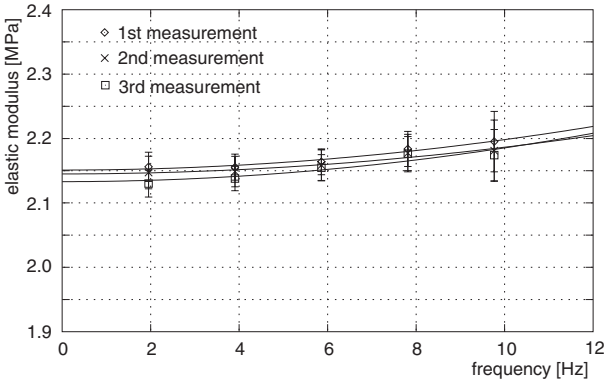

Fig. 7. Elastic moduli at each frequency measured for three trials. Vertical bars show standard deviations of elastic moduli measured for eleven beats.

ultrasonic measurements, was applied. Therefore, E_s obtained from the ultrasonic measurements and that from the mechanical test was slightly different. The string was produced by cutting the tube along the axial direction, and the sinusoidal stress was also applied along the axial direction by assuming isotropy.

From these results, the proposed method was shown to have a potential for estimating the viscosity of a cylindrical shell by applying frequency analysis to the change in wall thickness caused by the change in internal pressure.

5. Conclusions

In this study, we aimed to assess the viscosity of the arterial wall by frequency analysis of the change in wall thickness caused by the heartbeat in the late systole. Basic experiments using a silicone rubber tube were conducted to validate this approach. The change in internal pressure, which is similar to that at the human artery, was generated by a sophisticated flow pump, and the frequency analysis was applied to the measured changes in wall thickness and internal pressure. In the frequency range up to 10 Hz, in which the measured waveform had high reproducibility, the elastic modulus increased with frequency, and the viscosity constant was estimated from such measured frequency characteristics. These results show the potential of the proposed method for assessment of the viscosity of the arterial wall with ultrasound.

1) R. T. Lee, A. J. Grodzinsky, E. H. Frank, R. D. Kamm and F. J. Schoen: Circulation **83** (1991) 1764.
2) H. M. Loree, A. J. Grodzinsky, S. Y. Park, L. J. Gibson and R. T. Lee: J. Biomech. **27** (1994) 195.
3) P. C. G. Simons, A. Algra, M. L. Bots, D. E. Grobbee and Y. van der Graaf: Circulation **100** (1999) 951.
4) E. Falk, P. K. Shah and V. Fuster: Circulation **92** (1995) 657.
5) M. J. Davies: Circulation **94** (1996) 2013.
6) J. Golledge, R. M. Greenhalgh and A. H. Davies: Stroke **31** (2000) 774.
7) D. H. Bergel: J. Physiol. **156** (1961) 445.
8) L. H. Peterson, R. E. Jensen and J. Parnell: Circ. Res. **8** (1960) 622.
9) K. Hayashi, H. Handa, S. Nagasawa, A. Okumura and K. Moritake: J. Biomech. **13** (1980) 175.
10) A. P. G. Hoeks, C. J. Ruissen, P. Hick and R. S. Reneman: Ultrasound Med. Biol. **11** (1985) 51.
11) T. Länne, H. Stale, H. Bengtsson, D. Gustafsson, D. Bergqvist, B. Sonesson, H. Lecerof and P. Dahl: Ultrasound Med. Biol. **18** (1992) 451.
12) A. P. G. Hoeks, X. Di, P. J. Brands and R. S. Reneman: Ultrasound Med. Biol. **19** (1993) 727.
13) P. J. Brands, A. P. Hoeks, M. C. Rutten and R. S. Reneman: Ultrasound Med. Biol. **22** (1996) 895.
14) J. M. Meinders, P. J. Brands, J. M. Willigers, L. Kornet and A. P. G. Hoeks: Ultrasound Med. Biol. **27** (2001) 785.
15) H. Kanai, M. Sato, Y. Koiwa and N. Chubachi: IEEE Trans. UFFC **43** (1996) 791.
16) H. Kanai, H. Hasegawa, N. Chubachi, Y. Koiwa and M. Tanaka: IEEE Trans. UFFC **44** (1997) 752.
17) H. Hasegawa, H. Kanai, N. Chubachi and Y. Koiwa: Electron. Lett. **33** (1997) 340.
18) H. Hasegawa, H. Kanai, N. Chubachi and Y. Koiwa: Jpn. J. Med. Ultrason. **24** (1997) 851.
19) H. Hasegawa, H. Kanai, N. Hoshimiya, N. Chubachi and Y. Koiwa: Jpn. J. Appl. Phys. **37** (1998) 3101.
20) H. Kanai, K. Sugimura, Y. Koiwa and Y. Tsukahara: Electron. Lett. **35** (1999) 949.
21) H. Hasegawa, H. Kanai, N. Hoshimiya and Y. Koiwa: Jpn. J. Appl. Phys. **39** (2000) 3257.
22) H. Hasegawa, H. Kanai, N. Hoshimiya and Y. Koiwa: Jpn. J. Med. Ultrason. **28** (2001) 3.
23) H. Hasegawa, H. Kanai and Y. Koiwa: Jpn. J. Appl. Phys. **41** (2002) 3563.
24) H. Kanai, H. Hasegawa, M. Ichiki, F. Tezuka and Y. Koiwa: Circulation **107** (2003) 3018.
25) H. Hasegawa, H. Kanai, Y. Koiwa and J. P. Butler: Jpn. J. Appl. Phys. **42** (2003) 3255.
26) H. Hasegawa and H. Kanai: Jpn. J. Appl. Phys. **43** (2004) 3197.
27) M. Kondo, M. Ozawa, H. Kanai and N. Chubachi: Jpn. J. Med. Ultrason. **23** (1996) 271.
28) J. T. Young, R. S. Vaishnav and D. J. Patel: J. Biomech. **10** (1977) 549.
29) D. J. Patel, J. S. Janicki and R. N. Vaishnav: Circ. Res. **32** (1973) 93.